Thermorheological Effects of Long-Chain Branching in Entangled Polymer Melts

J. M. Carella,[1a] J. T. Gotro,[1b] and W. W. Graessley*[1c]

Departments of Chemical Engineering and Materials Science and Engineering, Northwestern University, Evanston, Illinois 60201. *Received July 9, 1985*

ABSTRACT: The dynamic modulus was measured over wide ranges of frequency and temperature for entangled melts of star branched polymers with a variety of microstructures—polyisoprene, polybutadiene of several vinyl contents, and their hydrogenation products. The data were examined for evidence of thermorheological complexity, and the temperature dependence of viscosity for linear and branched polymers with the same microstructure was compared. The temperature coefficients were found to be larger for branched polymers of some species. The excess was shown to be thermally activated, as opposed to the free volume activation that governs the temperature dependence for linear polymers. The activation energy is proportional to branch length and appears to be related to the temperature coefficient of chain dimensions for the species. The behavior was attributed to the different relaxation mechanisms for branched and linear chains in an entangled environment.

Introduction

The melt rheology of entangled polymers is strongly influenced by long-chain branching.[2-10] The terminal relaxation spectrum for nearly monodisperse star and comb polymers is much broader than the spectrum for linear polymers, and the laws that relate zero-shear viscosity and recoverable compliance to molecular weight are qualitatively different. Such departures from linear chain properties seem invariably to appear whenever the branches are long enough to be well entangled. They increase with branch length and decrease with dilution, eventually going over to the rather modest variations with chain architecture that typify dilute solution behavior. These effects of entanglement appear to be universal; explanations have been proposed based on the tube model and suppression of reptation by branch points.[10-15]

Entangled branches have other effects, however, that are clearly nonuniversal and have to do with thermorheological behavior. For entangled melts of linear chains the temperature dependence is remarkably simple. Time–temperature superposition works with considerable accuracy; i.e., the melts are *thermorheologically simple*, and the temperature coefficient of viscosity is independent of molecular weight.[5] Both these features carry over unchanged to branched polystyrene[7,8] and, with only minor variations, to branched polybutadiene,[6] but commercial polyethylene[16,17] and model polyethylene[18,19] with long branches behave quite differently. Time–temperature superposition no longer applies—the melts are *thermorheologically complex*—and the temperature coefficient of viscosity is elevated. Entanglement is certainly involved because the departures from linear polyethylene behavior closely parallel the other effects of entangled branches.[19] It has been proposed that these thermorheological variations among species are related to differences in the temperature coefficient of chain dimensions.[20] If so, the same departures from thermorheological simplicity should be seen in branched polymers other than polyethylene.

In the present paper we report an exploration of thermorheological effects for polymers with a wide range of chemical microstructures. Star branched polymers were prepared by anionic polymerization of isoprene and butadiene. Polybutadiene microstructures from ~8% to ~99% 1,2-vinyl content were obtained by the use of polymerization modifiers. The polymers were then hydrogenated to form a parallel series of saturated samples, corresponding in microstructure to copolymers of ethylene and 1-butene with 4%–99% 1-butene content (hydrogenated polybutadiene) and alternating copolymers of ethylene and propylene (hydrogenated 1,4-polyisoprene). Examples of both thermorheologically simple and complex behavior were found among these materials. The results are compared with the predictions about microstructural effects in branched polymers[20] with data on the linear homologues.[21,22]

Background

In entangled melts the viscosity and recoverable compliance of nearly monodisperse linear polymers vary with molecular weight according to[2,5,9]

$$\eta_0 = K_1 M^{3.4} \qquad M > M_c \tag{1}$$

$$J_e^0 \sim 2.5/G_N^0 \qquad M > M_c' \tag{2}$$

where K_1 depends on temperature and polymer species, and G_N^0 is the plateau modulus of the species. Typically, $M_c \sim 2M_e$ and $M_c' \sim 6M_e$, where M_e is the entanglement molecular weight[5]

$$M_e \equiv \rho RT/G_N^0 \tag{3}$$

and ρ is the melt density, R is the gas constant, and T is the temperature.

Star polymers in the same regime obey different laws[2,3,7]

$$\eta_0 = K_b \exp(\gamma M_a/M_e) \tag{4}$$

$$J_e^0 = K_b' M/\rho RT \tag{5}$$

where the exponential coefficient γ is of order unity and where K_b may depend on the arm molecular weight M_a and branch-point functionality f ($M = fM_a$) as well as temperature and species. The experimental values of K_b' are similar to those calculated with the Rouse–Ham equation for stars[7]

$$K_b' = \tfrac{2}{5}(15f - 14)/(3f - 2)^2 \tag{6}$$

The viscosity for stars below and even somewhat above the entanglement threshold is similar in magnitude to the viscosity for linear chains with the same radius of gyration. On the basis of that observation, Berry and Fox proposed a prefactor of the form[2]

$$K_b = [(3f - 2)M_a/f]^{3.4} K_1 \tag{7}$$

That relationship was used to establish viscosity enhancement factors (the exponential part of eq 4) for entangled stars.[2,3] Recent theory suggests a weaker prefactor dependence on molecular weight.[10,13,14] With $K_b \propto M_a^{1/2}$, $\gamma \sim 0.6$ was determined for polystyrene, polyisoprene, and polybutadiene stars with various branched-point functionalities.[10,23]

0024-9297/86/2219-0659$01.50/0

Zero-shear viscosity and recoverable compliance characterize the limiting response at low frequencies for the dynamic modulus $G^*(\omega) = G'(\omega) + iG''(\omega)$[5]

$$\eta_0 = \lim_{\omega \to 0} \frac{G''(\omega)}{\omega} \tag{8}$$

$$J_e^0 = \lim_{\omega \to 0} \frac{G'(\omega)}{[G''(\omega)]^2} \tag{9}$$

Over wide ranges of temperature the viscoelastic behavior of linear polymers obeys time–temperature superposition.[5,21,22] The response functions shift with temperature, but their forms remains essentially unchanged. Thus

$$G^*(\omega;T) = b_T G^*(a_T\omega;T_0) \tag{10}$$

where the reference temperature is T_0, and a_T and b_T are scale factors for frequency and modulus at T relative to T_0 ($a_{T_0} = b_{T_0} = 1$). For long chains the scale factors depend on microstructure but not on chain length. Moreover, the modulus scale factor is very insensitive to temperature.[5,21,22] As a result, J_e^0 and G_N^0 are practically independent of temperature, and to an excellent approximation

$$\eta_0(T) = a_T\eta_0(T_0) \tag{11}$$

As a result, the temperature dependence of viscoelastic response for linear chains of any microstructure is governed mainly by a_T, which is obtainable from data on $\eta_0(T)$. The values are well described by the WLF equation[5]

$$\log a_T = C_1^0(T - T_0)/(C_2^0 + T - T_0) \tag{12}$$

where C_1^0 and C_2^0 are independent of M. Values of a_T for the microstructures of interest here are reported in earlier publications.[21,22]

In polyethylene stars (hydrogenated stars of polybutadiene with low vinyl content) the form of $G^*(\omega)$ changes with temperature.[18] When $|G^*(\omega)|$ is large, the relaxations involve chain distances that are small compared with the branch length, and the shift in frequency scale with temperature is indistinguishable from that for linear polyethylene (hydrogenated linear polybutadiene with low vinyl content). As $|G^*(\omega)|$ decreases, the shifts begin to increase, growing as the corresponding chain distance increases and eventually reaching a maximum shift for the final relaxation of the molecules. We assume that the shift in modulus scale is negligible, some support for which is provided by the observation that J_e^0 for the same polymers is insensitive to temperature, as discussed below.

In effect, the frequency shift becomes a function of the modulus magnitude for polyethylene stars. The value of $(a_T)_B$ for stars, obtained from viscosity with eq 11, is larger than $(a_T)_L$, the viscosity shift factor for the linear polymer. Moreover, for polyethylene stars with different arm lengths[18,19]

$$\log [(a_T)_B/(a_T)_L] \propto M_a \tag{13}$$

The constant of proportionality turns out to be about 30% larger for four-arm stars than three-arm stars.

According to arguments advanced in ref 20, thermorheological complexity and enhanced temperature coefficients of viscosity should not be unique to branched polyethylene. These properties should appear for branched structures of any species in which the chain dimensions decrease with increasing temperature, i.e., when the temperature coefficient, $\kappa = \mathrm{d} \ln \langle R^2 \rangle / \mathrm{d}T$[24] is negative. Anomalous behavior for stars can be produced in two ways. First, if κ is negative and large, the plateau modulus will decrease with increasing temperature,[21,22,25] reducing the exponent in eq 4 by raising M_e. In this case, and aside from any mechanistic considerations, the viscosity of stars will fall more rapidly with temperature than linear polymers, and the disparity in temperature coefficient will increase with branch length, as observed (eq 13). Second, if the stars relax by arm retraction, a mechanism suggested by tube model considerations,[13-15] the transition states will have higher energy when κ is negative. This leads quite naturally to thermorheological complexity of the kind observed in branched polyethylene. It also produces an excess viscosity shift of the Arrhenius form

$$\ln [(a_T)_B/(a_T)_L] = E^*/RT + \text{const} \tag{14}$$

where E^* corresponds to the transition state energy for the longest relaxation time. Moreover, E^* should be directly proportional to arm length

$$E^* = \Lambda M_a/M_e \tag{15}$$

where the activation coefficient Λ depends only on polymer species and is governed by the same aspects of microstructure that determine κ.

If this explanation is correct, similar behavior should appear in other species where κ is negative and large, and departures from thermorheological simplicity should be absent or unobservable when κ is relatively small. (It is not clear what should happen when κ is positive or how κ and Λ are related in detail.) Furthermore, the excess temperature dependence for stars should behave like a thermally activated process (eq 14) even in the range where free volume (eq 12) governs the linear-chain behavior. That feature could not be tested with polyethylene because the $(a_T)_L$ data could be accommodated by either the WLF form or an Arrhenius equation over the available temperature range.[18,19] Some microstructures in the present study are more suitable for that test.

Experimental Procedures

Sample Preparation. Polybutadiene arms were made by anionic polymerization, moderated by small amounts of tetrahydrofuran to adjust the 1,2-vinyl content.[22] They were linked with $Si(CH_3)Cl_3$ or $SiCl_4$ (dropwise addition over a period to several hours) to form three-arm or four-arm stars.[6] The coupling efficiency was always high. Small amounts of uncoupled arms (~5%) were removed by fractionation. The polybutadiene stars with 99% vinyl content and all polyisoprene stars were made in benzene solution by vacuum-line techniques and generously supplied to us by L. J. Fetters.

The polymers were hydrogenated in cyclohexane solution with a $Pd/CaCO_3$ catalyst.[21,22] Hydrogenation of the three-arm and four-arm polybutadiene stars proceeded smoothly. Polyisoprene stars were more difficult, as had been noted also for linear polyisoprene.[21] Repeated hydrogenations were required to remove all detectable unsaturation. A small fraction of the polyisoprene stars was found to revert to arms during hydrogenation; a satellite peak corresponding to the arm always appeared in the GPC trace after hydrogenation (see Figure 1a) and was removed by fractionation. Fetters has also observed such "supernova" events (~4%) in polybutadiene stars,[26] but we find no indication of them in our samples (Figure 1b), perhaps owing to lower resolution in our GPC instrument.

Polybutadiene (PB) stars with more than four arms were generally more resistant to hydrogenation. It was sometimes necessary to repeat the hydrogenation with a fresh PB sample. However, all HPB stars used here had been hydrogenated only one time and were fully saturated according to infrared spectroscopy. The polyisoprene stars of higher functionality and one of the three-arm stars contained residual unsaturation even after repeated hydrogenation and were not used in the rheological studies.

Microstructure and Physical Properties. The fractions of 1,4 cis, 1,4 trans, and 1,2 units in the polybutadienes, the fractions of 3,4 units in the polyisoprenes (PI), and the residual unsaturation in the hydrogenated polybutadienes (HPB) and hydrogenated polyisoprenes (HPI) were determined by infrared

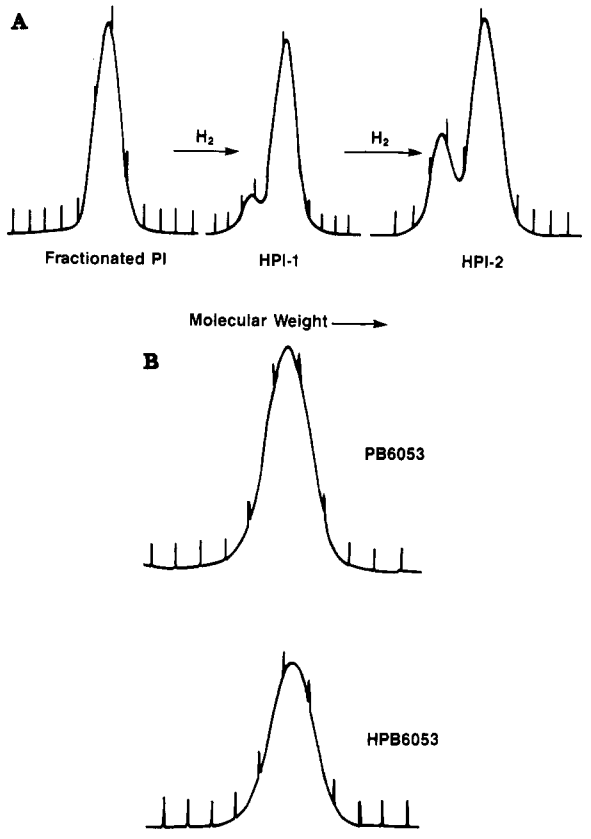

Figure 1. (A) Changes in the GPC trace for a polyisoprene star with successive hydrogenations. The shoulder corresponds in molecular weight to an unattached arm. (B) GPC traces for a three-arm polybutadiene star before and after hydrogenation.

spectroscopy.[21,22] The ratios of cis to trans units are similar to those of the corresponding linear polymers[21,22] at the same 1,2 or 3,4 levels. Residual unsaturation was below the limits of detectability in the HPB and HPI samples used in subsequent experiments. The glass transition temperature and density were measured on selected samples and found to be indistinguishable from values obtained for linear polymers with the same microstructure.[21,22]

All PI stars have the same microstructure, $x_{34} = 0.10 \pm 0.01$, a value which is slightly larger than $x_{34} = 0.08$ for the linear PI samples used in earlier work.[21] The HPI samples derived from them have the microstructure of strictly alternating ethylene/propylene copolymers, interrupted occasionally by isopropyl side groups.[21] The PB microstructures range from $x_{12} \sim 0.08$ to $x_{12} \sim 0.99$; the derived HPB samples correspond in microstructure to copolymers of ethylene and 1-butene (4%–99% 1-butene).[22] The microstructure and branch-point functionality are incorporated in the PB and HPB sample names; e.g., PB43S4 is a four-arm polybutadiene star with $x_{12} = 0.43$, and HPB43S4 is the product obtained by hydrogenation.

Molecular Weight and Distribution. The star polymers were characterized by a combination of methods, including those described earlier for the linear polymers.[21,22] Intrinsic viscosity was determined routinely for most samples in conjunction with gel permeation chromatography. The GPC results, corrected for axial dispersion, indicated narrow distributions in all samples, $\bar{M}_w/\bar{M}_n \lesssim 1.1$. Values of $\bar{M}_w$ were determined by light scattering, sometimes in line with GPC.[26] Arm molecular weights were determined by membrane osmometry or by GPC on samples withdrawn prior to coupling. The values obtained by different methods on the same sample, or by the same method before and after hydrogenation, were generally found to be in good agreement. Detailed comparisons of the results are available elsewhere.[27,28]

Table I summarizes the values obtained for the arm and total molecular weights. In most cases they are averages of values obtained by two or more methods. Only the HPI stars gave some difficulty in molecular weight assignment. We regard the values listed for those two cases, calculated from arm molecular weights for the PI precursors, to be the most reliable.

Table I
Molecular Weights for Star Polymers

sample	f	M_a	M	M_e
PIAS3	3	25 000	75 000	6 400
PIBS3	3	42 000	126 000	6 400
PICS3	3	60 000	180 000	6 400
PIDS12	12	70 000	840 000	6 400
PIES18	18	54 000	972 000	6 400
HPIBS3	3	43 000	129 000	1 860
HPICS3	3	62 000	186 000	1 860
PB08S3	3	26 000	76 000	2 030
PB25S4	4	43 000	171 000	6 350
PB43S4	4	33 000	127 000	2 660
PB60S3	3	42 000	122 000	3 420
PB80S3	3	98 000	290 000	4 440
PB99S3	3	70 000	225 000	5 210
PB99S8	8	70 000	580 000	5 210
PB99S18	18	69 000	1 200 000	5 210
HPB25S4	4	44 000	177 000	1 580
HPB43S4	4	33 000	132 000	2 310
HPB60S3	3	42 000	127 000	3 600
HPB80S3	3	100 000	301 000	6 300
HPB99S3	3	77 000	233 000	13 300
HPB99S8	8	75 000	600 000	13 300
HPB99S18	18	69 000	1 250 000	13 300

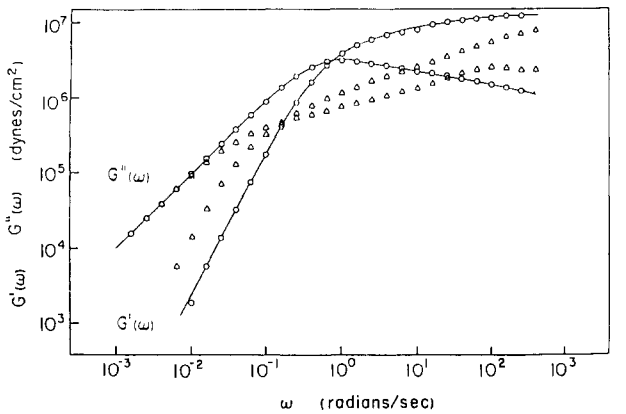

Figure 2. Comparison of dynamic moduli for a linear and a three-arm star hydrogenated polyisoprene at 50 °C. Lines are drawn through the data for the linear polymer (HPI – 1.115L[21] M = 163 000) (○). The branched polymer is HPIBS3, M = 126 000 (△). All data for the star polymer have been shifted to higher frequency (shift factor = $(\eta_0)_B/(\eta_0)_L = 1.48$) to coincide in $G''(\omega)$ at low frequencies with the linear polymer.

Rheological Measurements. Dynamic storage and loss moduli, $G'(\omega)$ and $G''(\omega)$, were obtained at frequencies in the range $0.001 < \omega < 250$ s^{-1} by the eccentric rotating disk method with a Rheometrics mechanical spectrometer. Data were gathered at several temperatures for each sample; wider ranges were generally accessible for the hydrogenated samples owing to their greater thermal stability. At some temperatures only low-frequency data were obtained; in others the full range of response was explored. A nitrogen atmosphere was used in all experiments. The samples were stabilized as described for the linear polymers;[21,22] the same procedures, corrections for instrumental compliance, and tests for thermal stability were employed. Viscosity and recoverable compliance were determined from the limiting response at low frequencies (eq 8 and 9) and are recorded in Table II.

General Observations

Dynamic Modulus. Dynamic moduli at 50 °C are shown in Figure 2 for a three-arm hydrogenated polyisoprene star (HPIBS3, $M = 126\,000$) and a linear polymer of similar microstructure (HPI-1.115L,[21] $M = 163\,000$). Both polymers are well entangled: M_e is 1860 for this microstructure.[21] Their viscosities are similar ($\eta_0 = 1.5_8 \times 10^7$ and $1.0_7 \times 10^7$ P, respectively); dynamic moduli for

Table II

a. Rheological Parameters for Polyisoprene Stars

sample	T, °C	η_0, P	$J_e^0 \times 10^6$, cm²/dyn	$(J_e^0)_R \times 10^6$,[a] cm²/dyn	sample	T, °C	η_0, P	$J_e^0 \times 10^6$, cm²/dyn	$(J_e^0)_R \times 10^6$,[a] cm²/dyn
PIAS3	25	2.1×10^4			PIDS12	25	8.1×10^6	2.6_5	2.16
PIBS3	25	$2.4_5 \times 10^5$	1.1_5	1.43		50	$1.6_5 \times 10^6$		
	50	4.7×10^4				75	$5.2_5 \times 10^5$		
	75	$1.5_5 \times 10^4$			PIES18	25	7.2×10^5	1.6_5	1.65
PICS3	25	$1.1_5 \times 10^6$	1.6_5	2.04		50	1.4×10^5		
	50	2.1×10^5				75	4.1×10^4		
	75	$6.7_5 \times 10^4$							

b. Rheological Parameters for Hydrogenated Polyisoprene Stars

sample	T, °C	η_0, P	$J_e^0 \times 10^6$, cm²/dyn	$(J_e^0)_B \times 10^6$,[b] cm²/dyn	sample	T, °C	η_0, P	$J_e^0 \times 10^6$, cm²/dyn	$(J_e^0)_B \times 10^6$,[b] cm²/dyn
HPIBS3	50	$1.5_8 \times 10^7$	1.5[a]	1.34	HPICS3	100	$3.9_8 \times 10^7$	2.0[a]	1.93
	75	$2.4_0 \times 10^6$				130	$7.5_9 \times 10^6$		
	100	$5.0_2 \times 10^5$				160	$2.1_4 \times 10^6$		
	130	$1.3_5 \times 10^5$				190	$7.2_4 \times 10^5$		

c. Rheological Parameters for Polybutadiene Stars

sample	x_{12}	T, °C	η_0, P	$J_e^0 \times 10^6$, cm²/dyn	$(J_e^0)_R \times 10^6$,[a] cm²/dyn	sample	x_{12}	T, °C	η_0, P	$J_e^0 \times 10^6$, cm²/dyn	$(J_e^0)_R \times 10^6$,[a] cm²/dyn
PB08S3	0.08	25	4.8×10^5	0.83	0.87	PB80S3	0.80	75	2.0×10^7		
		50	$1.3_8 \times 10^5$					100	4.2×10^6	4.0	2.64
		75	5.8×10^4			PB99S3	0.99	75	$1.2_5 \times 10^7$	2.2	2.20
PB25S4	0.25	25	$4.3_8 \times 10^6$					100	$1.6_7 \times 10^6$	2.0	
		50	$9.8_5 \times 10^5$					125	$3.6_6 \times 10^5$	2.3	
		75	$3.0_2 \times 10^5$					150	$1.1_5 \times 10^5$		
PB43S4	0.43	25	3.6×10^6	1.5	1.05			175	5.1×10^4		
		50	$7.2_5 \times 10^5$	1.4		PB99S8	0.99	75	$2.3_5 \times 10^7$	2.2_5	1.96
		75	$2.0_5 \times 10^5$	1.4				100	$2.5_7 \times 10^6$	2.1	
		100	$7.4_5 \times 10^4$					125	$5.2_5 \times 10^5$		
PB60S3	0.60	25	$2.0_9 \times 10^7$	1.4	1.39			150	$1.5_5 \times 10^5$		
		50	$2.3_4 \times 10^6$	1.3							
		75	$5.0_1 \times 10^5$	1.4							
		100	$1.6_5 \times 10^5$								
		125	6.9×10^4	1.0							
		150	3.8×10^4								

d. Rheological Parameters for Hydrogenated Polybutadiene Stars

sample	x_{12}	T, °C	η_0, P	$J_e^0 \times 10^6$, cm²/dyn	$(J_e^0)_R \times 10^6$,[a] cm²/dyn	sample	x_{12}	T, °C	η_0, P	$J_e^0 \times 10^6$, cm²/dyn	$(J_e^0)_R \times 10^6$,[a] cm²/dyn
HPB25S4	0.25	130	1.5×10^7			HPB80S3	0.80	75	1.9×10^7		
		160	$3.6_4 \times 10^6$					100	3.8×10^6	3.0	3.04
		190	$1.1_9 \times 10^6$					125	$1.0_7 \times 10^6$	2.9	
HPB43S4	0.43	75	$6.5_3 \times 10^6$					150	$4.0_3 \times 10^5$	2.9	
		100	$1.4_5 \times 10^6$	1.5	0.97	HPB99S3	0.99	50	$6.2_4 \times 10^6$		
		130	$3.4_6 \times 10^5$	1.6				75	$6.3_1 \times 10^5$	1.9	2.52
		160	1.1×10^5	1.5				100	$1.2_2 \times 10^5$	1.9	
		190	3.9×10^4					125	$3.4_7 \times 10^4$	1.8	
HPB60S3	0.60	50	2.1×10^7					150	$1.3_5 \times 10^4$	1.8	
		75	$3.1_6 \times 10^6$	1.6	1.38			175	$6.3_1 \times 10^3$		
		100	$7.1_6 \times 10^5$	1.5		HPB99S8	0.99	50	3.9×10^6		
		125	$2.1_4 \times 10^5$	1.5				75	$4.7_8 \times 10^5$	2.3	2.25
		150	$8.1_4 \times 10^4$					100	$8.9_1 \times 10^4$	2.3	
		175	3.64×10^4					125	$2.5_7 \times 10^4$	2.3	
		200	1.95×10^4					150	$1.0_4 \times 10^4$		
		225	1.07×10^4			HPB99S18	0.99	50	$8.6_3 \times 10^6$		
								75	$8.7_3 \times 10^5$	3.0	2.02
								100	$1.6_2 \times 10^5$	3.1	
								125	$4.6_7 \times 10^4$	3.0	
								150	$1.7_0 \times 10^4$		

[a] Calculated with eq 5 and 6. [b] Values of J_e^0 did not change detectably over the range of temperatures investigated.

the star were shifted slightly along the frequency axis to make $G''(\omega)$ at low frequencies coincide with the linear polymer values. The broader relaxation spectrum of the star is evident from the more gradual increase of $G'(\omega)$ toward the plateau modulus for that microstructure, $G_N^0 = 1.14 \times 10^7$ dyn/cm²,[21] and also by the nature of the $G''(\omega)$ peak, which is relatively sharp and well-defined for the linear polymer but broadened and displaced to much higher frequencies for the star. This difference in spectral shape is a general characteristic.[6,7,9,10] The terminal spectrum for entangled linear polymers assumes a relatively narrow and universal form, but the spectrum for entangled stars broadens progressively with increasing arm length.[9] The behavior of HPI stars is also thermorheologically complex, as discussed in more detail below.

Dynamic moduli are shown in Figure 3 for a three-arm hydrogenated polybutadiene star (HPB60S3, M = 127 000) at 75 °C for its polybutadiene precursor (PB60S3) at 50 °C. The viscosities are similar ($\eta_0 = 3.1_6 \times 10^6$ and $2.3_4 \times 10^6$ P); the HPB data were shifted in frequency scale

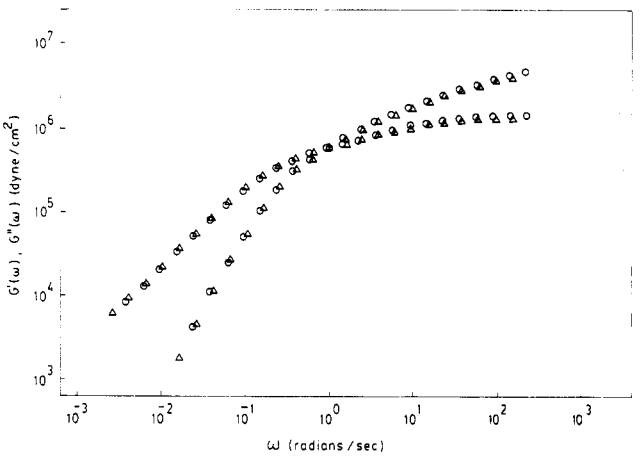

Figure 3. Comparison of storage moduli for a hydrogenated polybutadiene star (75 °C) and its polybutadiene precursor (50 °C). The symbols designate data for PB6053 (△) and HPB60S3 (○). All data for the HPB have been shifted to higher frequency (shift factor = $(\eta_0)_{HPB}/(\eta_0)_{PB}$ = 1.35) to coincide in $G''(\omega)$ at low frequencies with the PB star.

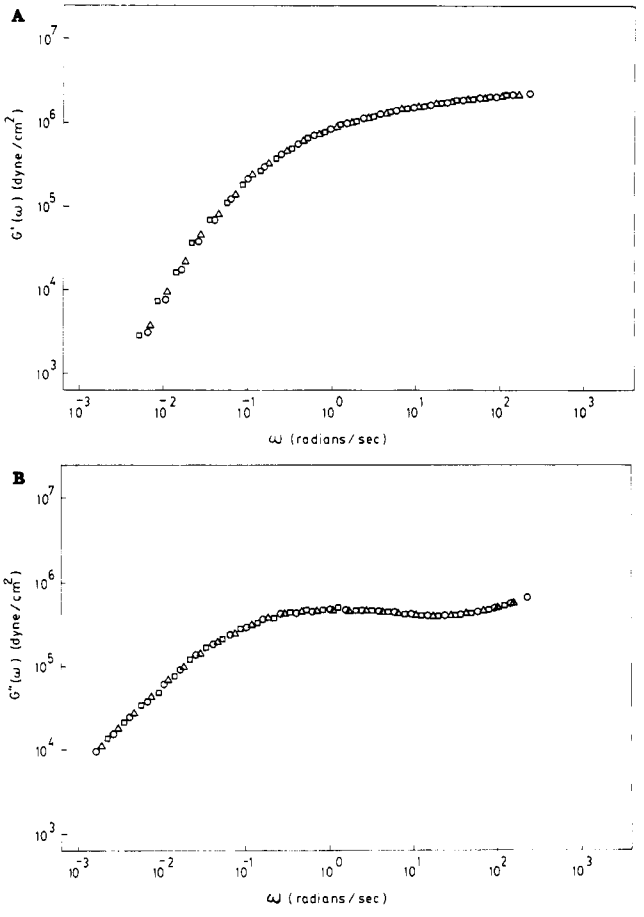

Figure 4. (A) Comparison of storage modulus master curves (T_0 = 50 °C) for hydrogenated polybutadiene stars with the same-arm molecular weight but different branch-point functionalities. The symbols designate data for HPB99S3 (○), HPB99S8 (△) and HPB99S18 (□). All data for the HPB99S8 have been shifted to lower frequency (shift factor = $(\eta_0)_8/(\eta_0)_3$ = 0.63) and for HPB99S18 to higher frequency (shift factor = $(\eta_0)_{18}/(\eta_0)_3$ = 1.38) to coincide in $G''(\omega)$ at low frequencies with the HPB99S3. (B) Comparison of loss modulus master curves for hydrogenated polybutadienes with the same-arm molecular weight but different branch-point functionalities. Sample designations and frequency shifts are the same as in A.

to obtain superposition in $G''(\omega)$ at low frequencies. When this adjustment is made, the agreement in both $G'(\omega)$ and $G''(\omega)$ is good except for very small departures at high

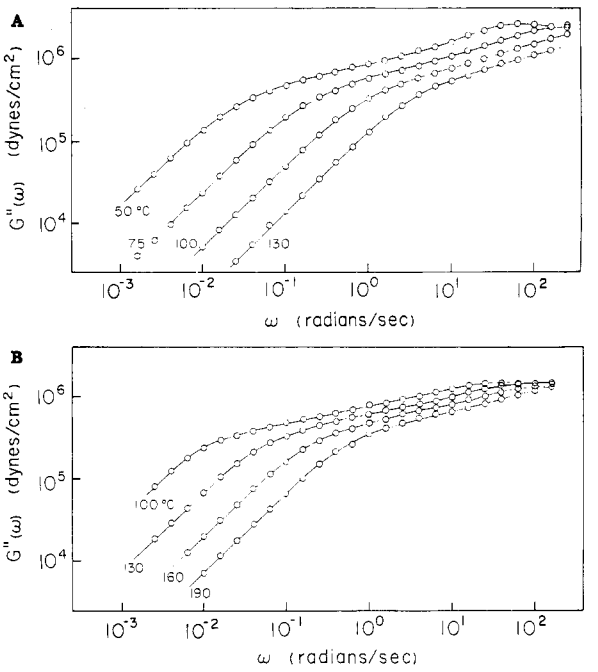

Figure 5. (A) Loss modulus for a hydrogenated polyisoprene three-arm star (M_a = 43 000) at several temperatures. (B) Loss modulus for a hydrogenated polyisoprene three-arm star (M_a = 62 000) at several temperatures.

frequencies. If these were linear polymers we would expect excellent superposition at all frequencies because PB and HPB with this microstructure (x_{12} = 0.60) have nearly the same plateau modulus ($G_N^0 \sim 0.7 \times 10^7$ dyn/cm²), making the two samples similar in both modulus scale and distance from the transition region.[22] The slight difference between the stars may be an effect of thermorheological complexity, as discussed below.

Dynamic moduli are shown in Figure 4 for HPB stars with the same microstructure (x_{12} = 0.99) and arm length ($M_a \sim$ 75 000) but different branch-point functionalities (f = 3, 8, and 18 for samples HPB99S3, HPB99S8, and HPB99S18). The response is thermorheologically simple for these stars: superposition of data obtained at different temperatures is excellent, and the shift factors are the same as those for the linear polymer.[22] The viscosities of the three stars are only slightly different; the composite of master curves (T_0 = 50 °C) shown in Figure 4 was formed by slight shifts to frequency scale for HPB99S8 and HPB99S18 to make $G''(\omega)$ coincide at low frequencies for all three stars. Agreement is excellent except in $G'(\omega)$ at low frequencies, reflecting a slight trend in J_e^0 with functionality. Apart from that, the behavior is consistent with recent theory which relates the terminal spectrum shape for stars to M_a/M_e alone.[10,13]

Loss moduli for the two HPI stars are shown for several temperatures in Figure 5. Both samples display thermorheological complexity of the kind observed earlier in polyethylene stars:[18,19] the shift with temperature in frequency scale increases with decreasing modulus. Shift factors for the loss modulus of HPIBS3 are shown as a function of G'' in Figure 6. Below $G'' \sim 1.5 \times 10^5$ dyn/cm² the loss modulus has reached its limiting form, $G'' \propto \omega$, at all temperatures. In that region the shift factors are independent of G'' and correspond to the viscosity shift $(a_T)_B$. The shift factors decrease progressively at higher modulus levels but become constant again beyond $G'' \sim 10^6$ dyn/cm². The values in that region agree fairly well with $(a_T)_L$, the viscosity shift factors for linear HPI.[21] Shift factors based on G' and $|G^*|$ behave in a similar fashion.

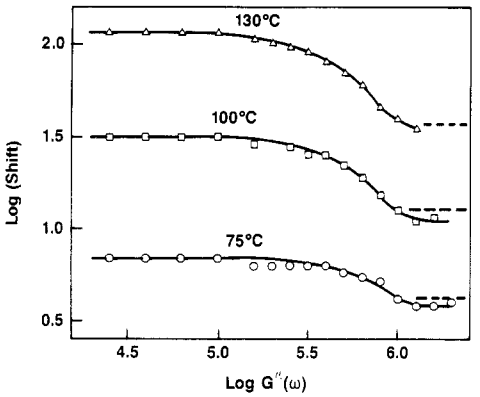

Figure 6. Temperature shift factor (T_0 = 50 °C) as a function of loss modulus magnitude for a hydrogenated polyisoprene three-arm star (HPIBS3). The modulus-independent shift factors for the linear polymer are shown by dashed lines.

The data for HPICS3 have the same general character, except that the difference between $(a_T)_B$ and $(a_T)_L$ is even larger than for HPIBS3.

In contrast with HPI, the polyisoprene stars show no evidence of thermorheological complexity. Temperature superposition is excellent, but the range, 25–75 °C, is probably too small for that to be a completely satisfactory test. In any case, the values of $(a_T)_B$ agree almost exactly with $(a_T)_L$ when adjusted for microstructural differences (x_{34} = 0.10 for the stars and x_{34} = 0.08 for the linear polymers).[21]

Viscosity. Viscosities of PI and HPI stars are compared with their linear chain counterparts in Figure 7. The Berry–Fox prefactor (eq 7) was used to display the data, so comparisons are made on the basis of a nominal molecular size.[2,3] (See ref 29 for a recent discussion of unperturbed chain dimensions in polymeric stars.) The PI stars show little enhancement of viscosity (Figure 7a). The HPI stars, on the other hand, have much larger viscosities than linear HPI's of the same nominal size (Figure 7b). This result is not surprising, however, in view of the difference in entanglement molecular weight: M_e = 6400 for PI and M_e = 1860 for HPI.[21] The exponential factor in eq 4 depends on M_a/M_e, and M_a/M_e is much larger for the hydrogenated polyisoprene stars (~23 for HPIBS3, ~33 for HPICS3) than the polyisoprene precursors (~6.6 for PIBS3, ~9.4 for PICS3).

Similar comparisons for PB and HPB stars (x_{12} = 0.99) at several temperatures are shown in Figure 8. The polymers have the same M_a but different functionalities. Viscosities are strongly enhanced at all temperatures for the PB stars but only moderately so in the HPB stars. Again, the entanglement molecular weight plays a major role (M_e = 5700 for PB (x_{12} = 0.99) and 13 300 for the corresponding HPB[22]). The exponent in eq 4 is smaller for the HPB stars (M_a/M_e ~ 5.6 compared with 12.3 for the PB stars), so a smaller viscosity enhancement is expected.

Differences between the two species in temperature dependence relative to linear polymers are also evident in Figure 8. Viscosities of HPB stars change with temperature in the same way as the linear polymers. For the PB precursors the star polymer viscosities change with temperature more rapidly than those for the linear polymers, and the values for the eight-arm star changes more rapidly than those for the three-arm star. Unlike their hydrogenated counterparts, the PB (x_{12} = 0.99) stars show evidence of thermorheological complexity.

Recoverable Compliance. Agreement between measured values of J_e^0 and those calculated with eq 5 and 6

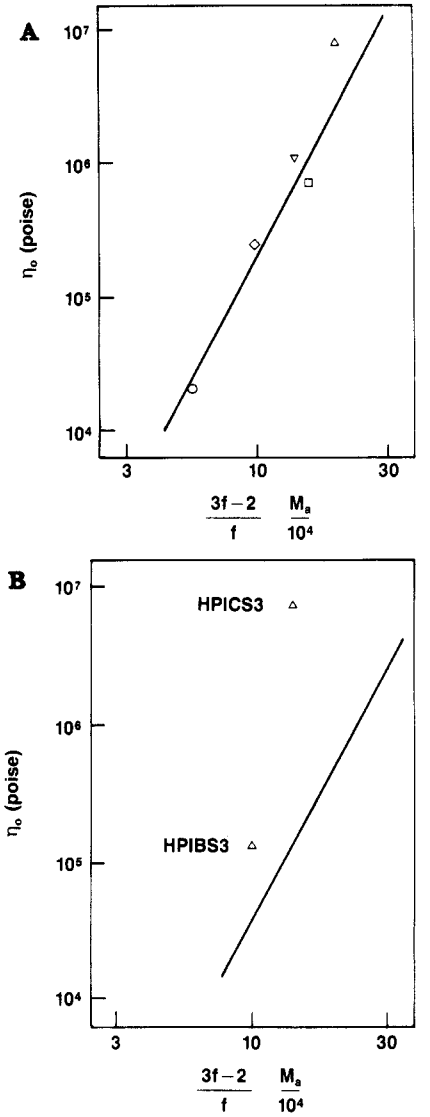

Figure 7. Comparison of viscosities for linear and star polyisoprenes at 25 °C on the basis of nominal molecular size. The line represented the data for linear polymers.[21] Symbols denotes PIAS3 (○), PIBS3 (◇), PICS3 (▽), PIDS12 (△), and PIES18 (□). (B) Comparison of viscosities for linear and star hydrogenated polyisoprenes at 100 °C on the basis of nominal molecular size. The line represents the data for linear polymers.[21]

(Table II) is reasonably good, as has been observed in other studies of star polymers.[6,7] The experimental values are insensitive to temperature even for polymers that clearly demonstrate thermorheological complexity, such as the HPI stars. This supports our interpretation that the change in shape of the modulus curves with temperature is due primarily to anomalous shifts in the relaxation times without significant change in the weighting factors. Any change in weighting factor for the longest relaxation times would cause variations of J_e^0 with temperature.[5]

Analysis of Temperature Dependence

Values of $(a_T)_B$ for the various microstructures were determined from the viscosities (Table II) with eq 11. Corresponding values of $(a_T)_L$ were obtained from viscosity data for linear polymers when available for the same or very similar microstructure or from the generalized correlations of $(a_T)_L$ and T_g with chain microstructure.[21,22] Figure 9 shows an Arrhenius plot of $(a_T)_B/(a_T)_L$ for the two three-arm HPI stars. Correction for the difference in microstructure of star (x_{34} = 0.10) and linear (x_{34} = 0.08) HPI has a negligible effect on the results. Reasonably good

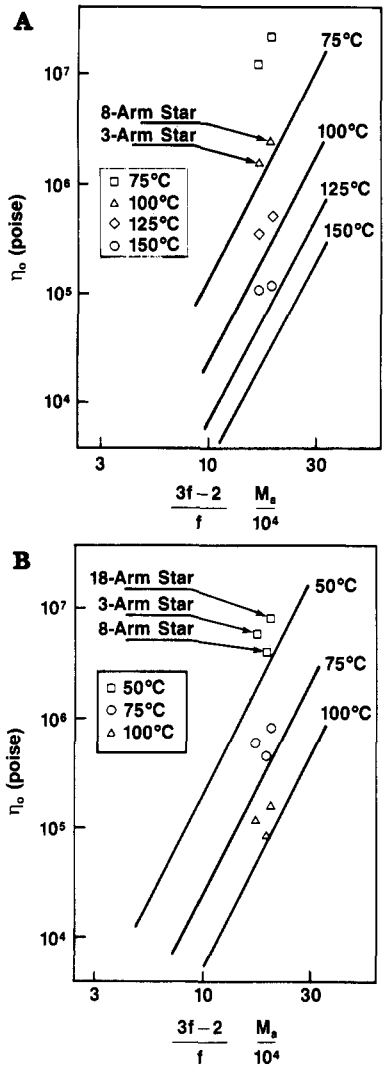

Figure 8. (A) Comparison of viscosities for linear and star polybutadienes (x_{12} = 0.99) at several temperatures. The lines represent the behavior for linear polymers (drawn with slopes of 3.4 and based on limited data[22]). (B) Comparison of viscosities for linear and star hydrogenated polybutadienes (x_{12} = 0.99) at several temperatures. See A.

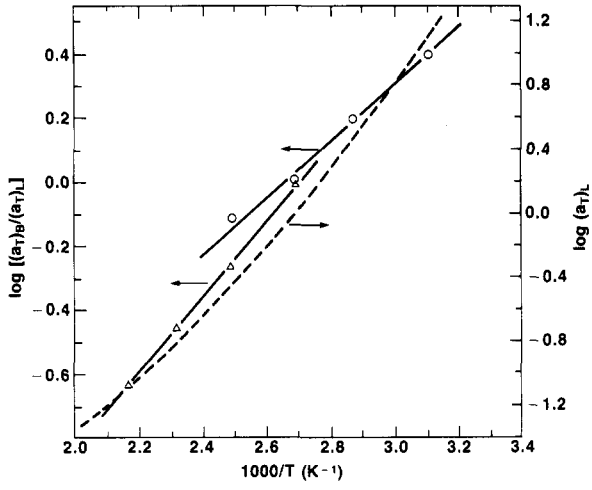

Figure 9. Arrhenius plots of shift factor ratio for hydrogenated polyisoprene stars. The dashed curve gives the shift factor for the linear polymer. The symbols denote data for HPIBS3 (○) and HPICS3 (△).

straight lines are obtained for both stars, which is consistent with expectations based on eq 14. The observations extend over ranges of temperature (50–130 °C and 100–190 °C) where an Arrhenius plot of $(a_T)_L$ alone, shown by the dashed line, is still somewhat curved. The activation energy E^* is different for the two stars (Table III) but roughly in proportion to arm length, as expected from eq 15.

Table III
Activation Energies in Star Polymers

sample	E^*, kcal	M_a/M_e	Λ, kcal
PIBS3	~0	6.6	0
PICS3	~0	9.5	0
PIDS12	~0	17.0	0
PIES18	~0	8.7	0
HPIBS3	4.0_2	23	0.17
HPICS3	5.3_8	33	0.16
PB08S3	1.3_6	12.8	0.11
PB25S4	2.6_2	18.3	0.14
PB43S4	2.0_0	12.4	0.16
PB60S3	2.1_7	12.3	0.18
PB80S3	2.9_8	22.1	0.13
PB99S3	2.1_5	12.3	0.17
PB99S8	3.5_7	12.3	0.29
HPB08S3	3–7	12–39	0.25[a]
HPB08S4	2–10	8–33	0.34[a]
HPB25S4	8.0_1	27.9	0.29
HPB43S4	4.2_5	14.3	0.30
HPB60S3	2.6_0	11.7	0.22
HPB80S3	1.5_8	15.9	0.10
HPB99S3	~0	5.8	0
HPB99S8	~0	5.6	0
HPB99S18	~0	5.2	0

[a] Average values of Λ obtained for three-arm and four-arm stars of HPB at x_{12} = 0.08[19] with M_e = 1250.

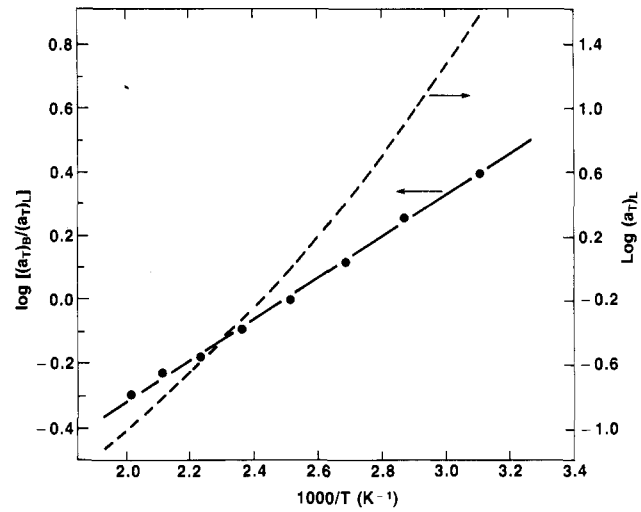

Figure 10. Arrhenius plot of the shift factor ratio for a hydrogenated polybutadiene star (HPB60S3). The dashed curve gives the shift factor for the linear polymer.

Figure 10 shows the results obtained for a three-arm star of hydrogenated polybutadiene with x_{12} = 0.60. Values of $(a_T)_L$ were obtained from viscosity data for HPB-1.965L,[22] a linear polymer of similar microstructure (x_{12} = 0.565). A WLF plot, $(T - T_0)/\log (a_T)_L$ vs. $T - T_0$, was used to extrapolate and interpolate the linear polymer results to the required temperatures. Adjustments were made to correct for the 1–2 °C difference in T_g from differences in microstructure.[22] As in HPI, the ΔT_g effect turns out to be negligible. This polymer provides a test of the Arrhenius form for $(a_T)_B/(a_T)_L$ over a very wide range of temperatures (50 ≤ T ≤ 225 °C), and the agreement is still reasonably good. In this range an Arrhenius plot of $(a_T)_L$ alone shows considerable curvature.

Figure 11 illustrates a more direct evaluation of E^*, in this case with PB60S3, the polybutadiene precursor of the

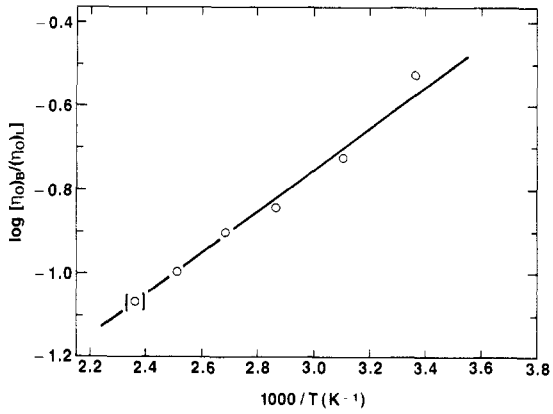

Figure 11. Arrhenius plot of the viscosity ratio for a linear and star polybutadiene of similar microstructure ($x_{12} \sim 0.60$).

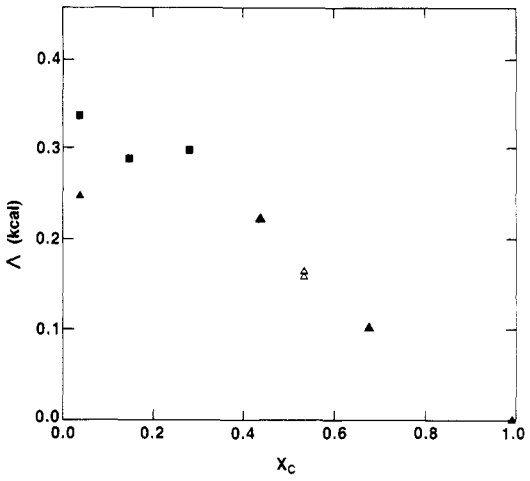

Figure 12. Activation coefficients for hydrogenated polyisoprene and hydrogenated polybutadiene as a function of microstructure. Symbols denote three-arm HPB (▲), three-arm HPI (△) and four-arm HPB (■); X_c denotes the equivalent mole fraction of counit in ethylene copolymer (see text).

polymer examined in Figure 10. The ratio of viscosities for a branched and linear polymer with the same microstructure varies with temperature in the same way as $(a_T)_B/(a_T)_L$; only the constant of proportionality depends on the large-scale structure of the two polymers. Thus, an Arrhenius plot of the viscosity ratio $(\eta_0)_B/(\eta_0)_L$ also gives E^*. Viscosity ratios were obtained from $\eta_0(T)$ for PB60S3 and PB1.965L,[22] the precursors of the polymers used to construct Figure 10. No correction for $\Delta T_g \sim 1$–2 °C was made in this case. Again, a straight line fits the data reasonably well.

Values of E^* were obtained for the other star polymers by procedures similar to those illustrated in Figures 9–11. In no case was serious curvature encountered, but smaller ranges of temperature were generally involved. Values of E^* and Λ (from eq 15) for the various microstructures, including earlier results from three-arm and four-arm stars of HPB ($x_{12} = 0.08$),[19] are listed in Table III.

Information on the temperature coefficient of chain dimensions is available for several species that closely resemble the ones examined here. Thus, hydrogenated polybutadiene ($x_{12} = 0.08$) is similar to polyethylene; $\kappa = -1.05 \times 10^{-3}$ °C^{-1} for polyethylene according to thermoelastic measurements on networks, dilute solution viscometry in athermal solvents, and rotational isomeric state (RIS) calculations.[30] Hydrogenated polybutadiene ($x_{12} = 0.99$) is equivalent to an ideally atactic poly(1-butene); $\kappa = +0.5 \times 10^{-3}$ °C^{-1} for atactic poly(1-butene) from thermoelastic measurements.[30] That value is also consistent with an analysis of $G_N^0(T)$ for linear HPB ($x_{12} = 0.99$).[22] Hydrogenated polyisoprene resembles an equimolar ethylene/propylene copolymer; $\kappa = -1.3 \times 10^{-3}$ °C^{-1} for a random copolymer near this composition according to thermoelastic measurments,[30] and the value is relatively insensitive to composition and sequencing according to RIS calculations.[31] Data on $G_N^0(T)$ for linear polybutadiene ($x_{12} = 0.99$)[22] suggest a large negative temperature coefficient for that species, $-10^3\kappa > 1$, but information from more standard methods is not available. The temperature coefficient for mixed microstructure polybutadiene ($x_{12} \sim 0.08$) is positive and moderate in magnitude, $\kappa = 0.39 \times 10^{-3}$ °C^{-1}, according to thermoelastic measurements.[32] A similar value, $\kappa = 0.3 \times 10^{-3}$ °C^{-1}, is expected for polyisoprene ($x_{34} = 0.1$), based on simple averaging of values for the high-cis and high-trans microstructures.[30]

From these data and the results in Table III, there is some indication of a rough correspondence between κ and Λ but nothing to suggest a simple proportionality. Thus, $\Lambda \sim 0$ for HPB ($x_{12} = 0.99$) and PI, and κ is positive for both species. Also, Λ is fairly large for HPB ($x_{12} \approx 0.08$), HPI, and PB ($x_{12} = 0.99$), and κ is large and negative for each but ordered differently than Λ. Finally, κ is positive for PB ($x_{12} = 0.08$), yet Λ is only marginally smaller than the values for species with large and negative κ. There is little evidence of a trend with microstructure in the PB stars. Moderate values of Λ are found at all vinyl contents. Differences in Λ between three-arm and higher arm stars, clearly evident for the HPB ($x_{12} = 0.08$) microstructure,[18,19] is seen also in PB ($x_{12} = 0.99$). Similar differences are present in the viscosity enhancement itself,[19] suggesting a weaker effect of branching for three-arm stars in general.

Systematic effects of microstructure are more evident in the hydrogenated polymers. Values of Λ for the HPB series are plotted in Figure 12 as a function of x_C, the mole fraction of 1-butene in the equivalent ethylene/1-butene copolymer:[33] $x_C = x_{12}/(2 - x_{12})$. Data for the HPI stars are also included, in this case using the mole fraction of total olefin counit with ethylene: "x_C" $= 1/(2 - x_{34}) = 0.53$ for $x_{34} = 0.10$. When a smaller effect in three-arm stars is allowed for, Λ appears to be roughly constant up to about 50% counit and then to decrease steadily toward 0 at $x_B \sim 1$.

These results show that branched polyethylene is by no means unique in displaying thermorheological complexity. Indeed, quite comparable values of Λ are found in other species as well. The effect is more prominent in polyethylene because the temperature coefficient of viscosity for the linear polymer is small, making the departures associated with E^* easy to observe. In addition, M_e is quite small in polyethylene, so departures develop even with arms of relatively low molecular weight ($M_a \sim 10^4$). On the other hand, the combination of large temperature coefficient of viscosity and large entanglement molecular weight may obscure such effects for species such as polystyrene, for which RIS calculations suggest a negative and perhaps relatively large value of κ.[34]

Summary and Conclusions

The relationship between thermorheological complexity and long-chain branching in polymer melts has been explored with a wide range of chain microstructures. Dynamic moduli were measured over a range of temperatures for regular stars of polybutadiene ($0.08 < x_{12} < 0.99$), polyisoprene ($x_{34} = 0.10$), and hydrogenated versions of the same polymers. Departures from time–temperature superposition and increased temperature coefficients of viscosity relative to linear chains were found for some

microstructures but not for others. The excess temperature dependence appears to depend on a thermally activated process rather than the free volume process that governs viscosity for linear polymers. The activation energies were used to estimate activation coefficients for the various species. A rough connection was established between these values and the temperature coefficient of chain dimensions for the species. For the saturated polymers, corresponding in microstructure to copolymers of ethylene, there appears to be a systematic relationship with the mole fraction of counit. The results are in general accord with expectations based on the difference in relaxation mechanisms available to entangled linear and branched polymers.

Acknowledgment. This work was supported by the National Science Foundation (CPE80-00030), the Northwestern University Materials Research Center (DMR-23573), the National Research Council of Argentina (CONICET), and a grant from Exxon Chemical Company. We are grateful to Gary VerStrate and L. J. Fetters for discussions, samples, and help with molecular characterization.

Registry No. Polyisoprene (homopolymer), 9003-31-0; polybutadiene (homopolymer), 9003-17-2.

References and Notes

(1) Current addresses: (a) Plapiqui, 8000 Bahia Blanca, Argentina; (b) IBM Corp., Systems Technology Division, Endicott NY 13760; (c) Corporate Research Laboratories, Exxon Research and Engineering Co., Annandale, NJ 08801.
(2) Berry, G. C.; Fox, T. G. *Adv. Polym. Sci.* **1968**, *5*, 261.
(3) Graessley, W. W. *Acc. Chem. Res.* **1977**, *19*, 332.
(4) Small, P. A. *Adv. Polym. Sci.* **1975**, *18*, 1.
(5) Ferry, J. D. "Viscoelastic Properties of Polymers", 3rd ed.; Wiley: New York, 1980.
(6) Rockefort, W. E.; Smith, G. G.; Rachapudy, H.; Raju, V. R.; Graessley, W. W. *J. Polym. Sci., Polym. Phys. Ed.* **1979**, *17*, 1197.
(7) Roovers, J.; Graessley, W. W. *Macromolecules* **1979**, *12*, 959.
(8) Roovers, J.; Graessley, W. W. *Macromolecules* **1981**, *14*, 766.
(9) Raju, V. R.; Menezes, E. J.; Marin, G.; Graessley, W. W.; Fetters, L. J. *Macromolecules* **1981**, *14*, 1668.
(10) Pearson, D. S.; Helfand, E. *Faraday Symp. Chem. Soc.* **1983**, *19*, 189; *Macromolecules* **1984**, *17*, 888.
(11) de Gennes, P.-G. *J. Phys. (Les Ulis, Fr.)* **1975**, *36*, 1199.
(12) Graessley, W. W.; Masuda, T.; Roovers, J.; Hadjichristidis, N. *Macromolecules* **1976**, *9*, 127.
(13) Doi, M.; Kuzuu, N. Y. *J. Polym. Sci., Polym. Lett. Ed.* **1980**, *18*, 775.
(14) Graessley, W. W. *Adv. Polym. Sci.* **1982**, *47*, 67.
(15) Klein, J.; Fletcher, D.; Fetters, L. J. *Faraday Symp. Chem. Soc.* **1983**, *18*, 159.
(16) Mendelson, R. A.; Bowles, W. A.; Finger, F. L. *J. Polym. Sci., Polym. Phys. Ed.* **1970**, *8*, 105.
(17) Rokadai, M., unpublished measurements.
(18) Raju, V. R.; Rachapudy, H.; Graessley, W. W. *J. Polym. Sci., Polym. Phys. Ed.* **1979**, *17*, 1223.
(19) Graessley, W. W.; Raju, V. R. *J. Polym. Sci., Polym. Symp.* **1984**, *No. 71*, 79.
(20) Graessley, W. W. *Macromolecules* **1982**, *15*, 1164.
(21) Gotro, J. T.; Graessley, W. W. *Macromolecules* **1984**, *17*, 2767.
(22) Carella, J. M.; Graessley, W. W.; Fetters, L. J. *Macromolecules* **1984**, *17*, 2775.
(23) Pearson, D. S., private communication.
(24) Flory, P. J. "Statistical Mechanics of Chain Molecules"; Interscience: New York, 1969.
(25) Graessley, W. W.; Edwards, S. F. *Polymer* **1981**, *22*, 1329.
(26) Fetters, L. J., private communication.
(27) Gotro, J. T. Ph.D. Thesis, Materials Science Department, Northwestern University, Evanston, IL, 1983.
(28) Carella, J. M. Ph.D. Thesis, Chemical Engineering Department, Northwestern University, Evanston, IL, 1983.
(29) Huber, K.; Burchard, W.; Fetters, L. J. *Macromolecules* **1984**, *17*, 541.
(30) Mark, J. E. *J. Polym. Sci., Macromol. Rev.* **1976**, *11*, 135; *Rubber Chem. Technol.* **1973**, *46*, 593.
(31) Mark, J. E. *J. Chem. Phys.* **1972**, *57*, 2541.
(32) Mark, J. E.; Llorente, M. A. *Polym. J. (Tokyo)* **1981**, *13*, 543.
(33) Krigas, T. M.; Carella, J. M.; Struglinski, M. J.; Crist, B.; Graessley, W. W.; Schilling, F. C. *J. Polym. Sci., Polym. Phys. Ed.* **1985**, *23*, 509.
(34) Yoon, D. Y.; Sundararajan, P. R.; Flory, P. J. *Macromolecules* **1975**, *8*, 776.

Examination of the Critical Parameters in the Constrained Junction Theory of Rubber Elasticity

R. W. Brotzman*† and J. E. Mark

IBM Research Laboratory, San Jose, California 95193. *Received June 26, 1985*

ABSTRACT: Stress–strain data previously obtained for a wide variety of unswollen and swollen polymer networks in elongation are interpreted by using the Flory–Erman theory of rubber elasticity. The interpretation is carried out as objectively as possible, with theoretical curves chosen on the basis of minimum residuals between theory and experiment and with realistic estimates of the uncertainties involved. High-elongation values of the reduced stress obtained from the theoretical curves were found to be very nearly independent of the degree of swelling. They differed significantly, in some cases, from the intercepts ($2C_1$) obtained by simple linear extrapolations of the data. Low-elongation values, however, are quite close to the linearly extrapolated values. In the theory employed, the reduced stress depends on the extent to which junction fluctuations are constrained, which in turn depends on the degree of interpenetration of the chain configurational domains. Values of an interpenetration parameter, although defined to account for the configurational characteristics of the chains investigated, were unfortunately found to show some dependence on the degree of swelling and the nature of the elastomeric chains.

Introduction

The most general molecular theory of rubber elasticity treats both "phantom" networks (in which the chains can transect one another and cross-links can fluctuate freely) and real networks (in which chain entangling constrains these fluctuations).[1-3] It has been used with considerable success in interpreting stress–strain measurements, in particular the elongation dependence of the reduced stress defined by

$$[f^*] = f^*(V/V^\circ)^{-1/3}(\alpha - \alpha^{-2})^{-1} \quad (1)$$

where f^* is the tensile force per unit area in the reference

†Current address: Department of Chemistry/CUNY, Staten Island, NY 10301.

0024-9297/86/2219-0667$01.50/0